arXiv:1401.7919v2 [quant-ph] 20 Mar 2014

Robust construction of entangled coherent GHZ and W states in a cavity QED system

N. Behzadi [a] *, B. Ahansaz [b] †, S. Kazemi [b] ‡

[a]Research Institute for Fundamental Sciences,

[b]Department of Theoretical Physics and Astrophysics, Faculty of Physics,

University of Tabriz, Tabriz 51666-16471, Iran.

March 24, 2014

Abstract

By exploiting a system of three distant cavities, we propose a scheme for constructing tripartite entangled coherent GHZ and W states which are robust due to the photon losses in the cavities. Each of cavities is doped with a semiconductor quantum dot. By the dynamics, the excitonic modes of quantum dots are enabled to exhibit entangled coherent GHZ and W states. Apart from the exciton losses, the master equation approach shows that when the populations of the field modes in the cavities are negligible the destruction of entanglement due to decoherence arises from photon losses, is effectively suppressed.

PACS Nos: 03.65.Ud, 03.65.Fd
Keywords: GHZ-state and W-state, Coherent states, Tripartite entanglement, Decoherence, Master equation

1 Introduction

Cavity quantum electrodynamics (QED) provides a natural setting for distributed quantum information processing (QIP) [1]. One requirement of distributed QIP is the coupling of distant qubits in order to perform state transfer, entanglement generation, or quantum gate operations between separate nodes of the system. Coupled cavities not only can be considered as a tool for observing of quantum cooperative phenomena in strongly correlated many-body systems [2] and also in observing strong coupling between photons and qubits inside the cavities [3, 4] but also has potential applications in QIP [5]. Recently, considerable theoretical efforts have been devoted to a class of coupled-cavity models that promise to

*E-mail:n.behzadi@tabrizu.ac.ir
†E-mail:bahramahansaz88@ms.tabrizu.ac.ir
‡E-mail:s.kazemirudsary89@ms.tabrizu.ac.ir

overcome the problem of individual addressability which is a difficult task in spin models [6]. Furthermore, the interaction of a cavity and an atom can be engineered in such way that the atom trapped in the cavity can have relatively long-lived energy levels which is suitable for various QIP protocols such as entanglement generations [7]. Indeed, the system of high-Q cavities and atoms, or specifically semiconductor quantum dots (QDs) as artificial atoms, in the strong interaction regime is one of experimentally realizable systems in which the intrinsic quantum mechanical coupling dominates losses arisen due to dissipation [6-8]. For example, in recent years, various schemes based on cavity QED systems have been proposed to generate entanglement between atoms or QDs trapped in distant optical coupled cavities which would be required for distributed quantum computing [9-13].

The discovery that tripartite entanglement can provide a stronger violation of local realism [16, 17] than bipartite entanglement has triggered a large research activity with the aim to generate it and find its applications. For example, generating tripartite entanglement between three atoms trapped in three distant cavities connected by optical fibers via quantum Zeno dynamics has been proposed in [18, 19]. In [20], deterministically generating tripartite entangled states of distant atoms based on the selective photon emission and absorption processes, using three cavities linked by optical fibers, has been discussed. It has become clear that for the system shared by three parties there are two inequivalent classes of entangled states, i.e., the GHZ state and the W state [21] found applications in realizing quantum information processing tasks [22]. Furthermore, the entangled coherent states (ECSs) [23] have emerged as a genuinely useful set of entangled states having a prominent role, for instance, in quantum teleportation and quantum computing [22-24] so, in the same way, have did entangled coherent GHZ and W states [27, 28].

In this work, we propose a protocol for generating tripartite entangled coherent GHZ and W states by exploiting three coupled-cavity QED which each of them is doped with a QD strongly coupled to it. We show that if excitonic mode of one of QDs is prepared in an even or odd coherent state and the other QDs and cavities are in their respective vacuum states, the dynamics of the system, at a characteristic time, layouts entanglement for the standard coherent states associated to excitonic modes of three distant noninteracting QDs. To evaluate the similarity of the generated entangled coherent states to coherent GHZ and W states quantitatively, we exploit GHZ state-based and W state-based entanglement witnesses (EWs) introduced in [29, 30]. Also, in this way, the process of constructing tripartite entanglement of coherent GHZ and W states is established in such a way that the effect of decoherence arisen almost from photon loss in cavities becomes negligible. In the resonance interaction between the field mode of cavities and the respective excitonic mode of the QDs, the field mode extremely populates, which in turn, leads to decay of photons and therefore lose of coherency of the system [31, 32]. It is shown that, when the field mode is highly detuned with the excitonic mode, the establishment of entanglement can be satisfied without populating the field mode in the cavities. Therefore, by the master equation approach, the proposed protocol for constructing entanglement, apart from the exciton losses, is robust to decoherence arisen from photon loss and thus, the efficient decoherence rate of the cavities is greatly prolonged.

This paper is laid out in the following way. In section 2, we describe the basic properties of the scheme. In Section 3, we are going to describe the realization of the scheme and represent a mechanism for dominating on the decoherence influencing the system to lose its

coherency. The paper is ended with a brief conclusion.

2 Hamiltonian and dynamics

We consider three QDs trapped in the three separated equidistance single-mode cavities placed at the vertices of a equilateral triangle as depicted in Fig. 1. The size of each QD satisfies the condition $R \gg a_B$ (Bohr radius). It is assumed that in the quantum dots there are a few electrons excited from valanced-band to conduction-band and the excitation density of the Coulomb correlated electron-hole pairs, excitons, in the ground state for each quantum dot is low. This, in fact, indicates that the average number of excitons is no more than one for an effective area of the excitonic Bohr radius. Consequently, exciton operators can be approximated with boson operators. Also, all nonlinear terms including exciton-exciton interactions and the phase-space filling effect can be neglected. It is also assumed that the ground energy of the excitons in each quantum dot is the same. The Hamiltonian Under the rotating wave approximation is given by

$$\hat{H} = \hbar\omega_c \sum_{i=1}^{3} \hat{a}_i^\dagger \hat{a}_i + \hbar\omega_e \sum_{i=1}^{3} \hat{b}_i^\dagger \hat{b}_i + \hbar g \sum_{i=1}^{3} (\hat{b}_i^\dagger \hat{a}_i + \hat{b}_i \hat{a}_i^\dagger) + \hbar c \sum_{i=1}^{3} (\hat{a}_i^\dagger \hat{a}_{i+1} + \hat{a}_{i+1}^\dagger \hat{a}_i), \qquad (1)$$

where $a_i^\dagger$ (a_i) is the creation (annihilation) operator for the ith ($4 \equiv 1$mode3) cavity field mode with frequency w_c and $b_i^\dagger$ (b_i) is the creation(annihilation) operator for the ith excitonic mode with frequency w_e. The coupling constants between quantum dot and cavity field are represented by g and the coupling strength between the cavities is c, which in turn, depends strongly on both the geometry of the cavities and the actual overlap between adjacent cavities. By assuming $\hbar = 1$ and $\omega_e = \omega_c - \Delta$, the Heisenberg equations of motion for the operators of cavities field and excitons lead to the first order differential matrix equation as follows

$$\begin{pmatrix} \dot{\hat{a}}_1 \\ \dot{\hat{a}}_2 \\ \dot{\hat{a}}_3 \\ \dot{\hat{b}}_1 \\ \dot{\hat{b}}_2 \\ \dot{\hat{b}}_3 \end{pmatrix} = -i \begin{pmatrix} \omega_c & c & c & g & 0 & 0 \\ c & \omega_c & c & 0 & g & 0 \\ c & c & \omega_c & 0 & 0 & g \\ g & 0 & 0 & \omega_c - \Delta & 0 & 0 \\ 0 & g & 0 & 0 & \omega_c - \Delta & 0 \\ 0 & 0 & g & 0 & 0 & \omega_c - \Delta \end{pmatrix} \begin{pmatrix} \hat{a}_1 \\ \hat{a}_2 \\ \hat{a}_3 \\ \hat{b}_1 \\ \hat{b}_2 \\ \hat{b}_3 \end{pmatrix}. \qquad (2)$$

Solving this equation is very simple and so, in this way, $\hat{b}_1(t)$ is written as below and the other operators have been inserted in the appendix.

$$\hat{b}_1(t) = u_{21}(t)\hat{a}_1(0) + u_{22}(t)\left(\hat{a}_2(0) + \hat{a}_3(0)\right) + v_{21}(t)\hat{b}_1(0) + v_{22}(t)(\hat{b}_2(0) + \hat{b}_3(0)), \qquad (3)$$

where $u_{2j}(t)$ and $v_{2j}(t)$ for $j=1,2$ are denoted as

$$\begin{aligned}
u_{21}(t) &= \tfrac{ie^{-i\omega_c t}}{6}\left(e^{-i(c-\frac{\Delta}{2})t}(-A+\tfrac{(2c+\Delta)^2}{A})sin(\tfrac{At}{2}) - 2e^{i(\frac{c+\Delta}{2})t}(B-\tfrac{(c-\Delta)^2}{B})sin(\tfrac{Bt}{2})\right),\\
u_{22}(t) &= \tfrac{ie^{-i\omega_c t}}{6}\left(e^{-i(c-\frac{\Delta}{2})t}(-A+\tfrac{(2c+\Delta)^2}{A})sin(\tfrac{At}{2}) + e^{i(\frac{c+\Delta}{2})t}(B-\tfrac{(c-\Delta)^2}{B})sin(\tfrac{Bt}{2})\right),\\
v_{21}(t) &= \tfrac{e^{-i\omega_c t}}{3}\left(e^{-i(c-\frac{\Delta}{2})t}(cos(\tfrac{At}{2})+\tfrac{i(2c+\Delta)}{A}sin(\tfrac{At}{2})) + 2e^{i(\frac{c+\Delta}{2})t}(cos(\tfrac{Bt}{2})-\tfrac{i(c-\Delta)}{B}sin(\tfrac{Bt}{2}))\right),\\
v_{22}(t) &= \tfrac{e^{-i\omega_c t}}{3}\left(e^{-i(c-\frac{\Delta}{2})t}(cos(\tfrac{At}{2})+\tfrac{i(2c+\Delta)}{A}sin(\tfrac{At}{2})) - e^{i(\frac{c+\Delta}{2})t}(cos(\tfrac{Bt}{2})-\tfrac{i(c-\Delta)}{B}sin(\tfrac{Bt}{2}))\right),
\end{aligned} \tag{4}$$

in which $A=\sqrt{4c^2+4c\Delta+\Delta^2+4g^2}$ and $B=\sqrt{c^2-2c\Delta+\Delta^2+4g^2}$. We assume that the excitonic mode of the first QD is prepared initially in a superposition of two distinct coherent states $|\alpha_1\rangle$ and $|\alpha_2\rangle$ and the other excitonic and field modes are at their respective vacuum states so the initial state of the whole system is written as

$$|\psi(0)\rangle = \frac{1}{\sqrt{N}}\,|0\rangle_{c_1}|0\rangle_{c_2}|0\rangle_{c_3}\left(|\alpha_1\rangle + e^{i\theta}|\alpha_2\rangle\right)_{e_1}|0\rangle_{e_2}|0\rangle_{e_3}, \tag{5}$$

where $N=(2+2cos(\theta+Im(\alpha_1^*\alpha_2))\,e^{-1/2(|\alpha_1|^2+|\alpha_2|^2)+Re(\alpha_1^*\alpha_2)}$ is the normalization coefficient and $|\alpha\rangle := e^{\alpha\hat{a}^\dagger(0)-\alpha^*\hat{a}(0)}|0\rangle$ is defined as a standard coherent state. The subscripts c and e stand for cavity and exciton modes respectively. Time evolution of the initial state is obtained as

$$\begin{aligned}
|\psi(t)\rangle = \frac{1}{\sqrt{N}}(&|\alpha_1 u_{21}(t)\rangle_{c_1}\otimes|\alpha_1 u_{22}(t)\rangle_{c_2}\otimes|\alpha_1 u_{22}(t)\rangle_{c_3}\otimes|\alpha_1 v_{21}(t)\rangle_{e_1}\otimes|\alpha_1 v_{22}(t)\rangle_{e_2}\otimes|\alpha_1 v_{22}(t)\rangle_{e_3}\\
+e^{i\theta}&|\alpha_2 u_{21}(t)\rangle_{c_1}\otimes|\alpha_2 u_{22}(t)\rangle_{c_2}\otimes|\alpha_2 u_{22}(t)\rangle_{c_3}\otimes|\alpha_2 v_{21}(t)\rangle_{e_1}\otimes|\alpha_2 v_{22}(t)\rangle_{e_2}\otimes|\alpha_2 v_{22}(t)\rangle_{e_3}).
\end{aligned} \tag{6}$$

The reduced density operator for the excitonic modes of three QDs is found as

$$\begin{aligned}
\hat{\rho}_e(\theta,\alpha_1,\alpha_2;t) = \tfrac{1}{N}(&|\alpha_1 v_{21}(t),\alpha_1 v_{22}(t),\alpha_1 v_{22}(t)\rangle\langle\alpha_1 v_{21}(t),\alpha_1 v_{22}(t),\alpha_1 v_{22}(t)|\\
&+|\alpha_2 v_{21}(t),\alpha_2 v_{22}(t),\alpha_2 v_{22}(t)\rangle\langle\alpha_2 v_{21}(t),\alpha_2 v_{22}(t),\alpha_2 v_{22}(t)|\\
&+q_1(t)q_2(t)^2 e^{-i\theta}|\alpha_1 v_{21}(t),\alpha_1 v_{22}(t),\alpha_1 v_{22}(t)\rangle\langle\alpha_2 v_{21}(t),\alpha_2 v_{22}(t),\alpha_2 v_{22}(t)|\\
&+q_1^*(t)q_2^*(t)^2 e^{i\theta}|\alpha_2 v_{21}(t),\alpha_2 v_{22}(t),\alpha_2 v_{22}(t)\rangle\langle\alpha_1 v_{21}(t),\alpha_1 v_{22}(t),\alpha_1 v_{22}(t)|),
\end{aligned} \tag{7}$$

where $q_1(t)=e^{-1/2(|\alpha_1|^2+|\alpha_2|^2-2\alpha_2^*\alpha_1)|u_{21}|^2}$ and $q_2(t)=e^{-1/2(|\alpha_1|^2+|\alpha_2|^2-2\alpha_2^*\alpha_1)|u_{22}|^2}$. It is evident that, by the dynamics, the reduced density operator for the excitonic modes becomes, in general, mix.

3 Entanglement

Let us consider $\alpha_1 = -\alpha_2 = \alpha$, the density matrix $\hat{\rho}(\theta, \alpha; t)$ in (7) becomes as

$$\begin{aligned}\hat{\rho}(\theta,\alpha;t) = \tfrac{1}{N}(&|\alpha v_{21}(t), \alpha v_{22}(t), \alpha v_{22}(t)\rangle \langle \alpha v_{21}(t), \alpha v_{22}(t), \alpha v_{22}(t)| \\ &+ |-\alpha v_{21}(t), -\alpha v_{22}(t), -\alpha v_{22}(t)\rangle \langle -\alpha v_{21}(t), -\alpha v_{22}(t), -\alpha v_{22}(t)| \\ &+ q_1(t)q_2(t)^2(e^{-i\theta} |\alpha v_{21}(t), \alpha v_{22}(t), \alpha v_{22}(t)\rangle \langle -\alpha v_{21}(t), -\alpha v_{22}(t), -\alpha v_{22}(t)| \\ &+ e^{i\theta} |-\alpha v_{21}(t), -\alpha v_{22}(t), -\alpha v_{22}(t)\rangle \langle \alpha v_{21}(t), \alpha v_{22}(t), \alpha v_{22}(t)|)),\end{aligned} \tag{8}$$

One can always rebuild two orthogonal and normalized states as basis of the two-dimensional Hilbert space using original two nonorthogonal coherent states, i.e.

$$\begin{aligned}|\alpha v_{21}(t)\rangle &:= |0\rangle, \quad |-\alpha v_{21}(t)\rangle := p_1(t)|0\rangle + \sqrt{1-p_1^2(t)}\,|1\rangle, \\ |\alpha v_{22}(t)\rangle &:= |0\rangle, \quad |-\alpha v_{22}(t)\rangle := p_2(t)|0\rangle + \sqrt{1-p_2^2(t)}\,|1\rangle,\end{aligned} \tag{9}$$

where $|0\rangle$ and $|1\rangle$ are orthogonal basis and $p_1(t) = e^{-2|\alpha|^2|v_{21}(t)|^2}$ and $p_2(t) = e^{-2|\alpha|^2|v_{22}(t)|^2}$. By rewritten the nonorthogonal basis of the density matrix $\hat{\rho}(\theta, \alpha; t)$ in terms of the orthogonal ones $|0\rangle$ and $|1\rangle$ the density matrix $\hat{\rho}(\theta, \alpha; t)$ is encoded as a three qubit quantum state, so the detect of generated entanglement between excitonic modes in three QDs becomes as the detection of entanglement in three-qubit quantum states. To this aim, we exploit EWs introduced in [29, 30]. At first, we consider the GHZ state-based EW as follows

$$\hat{W} = \frac{1}{2}1 \otimes 1 \otimes 1 - |GHZ\rangle \langle GHZ|. \tag{10}$$

where $|GHZ\rangle = \frac{1}{\sqrt{2}}(|000\rangle + |111\rangle)$ is the famous GHZ-state and $1/2$ is the maximal squared overlap between $|GHZ\rangle$ and the convex set of biseparable states. The expectation values of $\hat{W}$ with respect to $\hat{\rho}(\theta, \alpha; t)$, after encoding as a three qubit density matrix, is as

$$E_{_{GHZ}}(\hat{\rho}(\theta,\alpha;t)) \equiv Tr(\hat{W}\hat{\rho}(\theta,\alpha;t)) = \tfrac{1}{2} - F(|GHZ\rangle\langle GHZ|, \hat{\rho}(\theta,\alpha;t))^2 \tag{11}$$

where $F(|GHZ\rangle\langle GHZ|, \hat{\rho}(\theta, \alpha; t)) = \sqrt{\langle GHZ|\hat{\rho}(\theta,\alpha;t)|GHZ\rangle}$ is the fidelity between $\hat{\rho}(\theta, \alpha; t)$ and the GHZ-state. It appears that for density operator $\hat{\rho}(\theta = 0, 2; t)$ the expectation values of the witness operator $\hat{W}$ for some times t^* becomes very close to -1/2, that is, $F(|GHZ\rangle\langle GHZ|, \hat{\rho}(0, 2; t^*)) \simeq 1$. This shows that when the value of α is sufficiently large (for example is 2), the state $\hat{\rho}(0, 2; t)$ of the three excitonic modes approaches to the GHZ-state as shown in Fig. 2 and Fig. 3, and so the entanglement of $\hat{\rho}(0, 2; t)$ can be considered as entanglement of coherent GHZ-state [33]. Also, we can obtain the average number of photons in the cavity field modes as follows

$$\langle n_c \rangle = \frac{(1 - e^{-2|\alpha|^2})|\alpha|^2(|u_{21}(t)|^2 + 2|u_{22}(t)|^2)}{1 + e^{-2|\alpha|^2}}, \tag{12}$$

where it has been depicted in Fig. 2 and Fig. 3, for resonance interaction between photon and exciton and nonresonance one respectively.

In the next step, we consider W state-based EW [29, 30] as

$$\hat{W}' = \frac{2}{3}1 \otimes 1 \otimes 1 - |W\rangle \langle W|, \tag{13}$$

where $|W\rangle = \frac{1}{\sqrt{3}}(|001\rangle + |010\rangle + |100\rangle)$ is the W-state and 2/3 corresponds to the maximal squared overlap between $|W\rangle$ and the set of biseparable states B. Expectation values of the witness operator $\hat{W}'$ with respect to the $\hat{\rho}(\theta, \alpha; t)$ yields as

$$E_W\left(\hat{\rho}(\theta, \alpha; t)\right) \equiv Tr(\hat{W}'\hat{\rho}(\theta, \alpha; t)) = \frac{2}{3} - F(|W\rangle\langle W|, \hat{\rho}(\theta, \alpha; t))^2, \tag{14}$$

where $F(|W\rangle\langle W|, \hat{\rho}(\theta, \alpha; t)) = \sqrt{\langle W|\hat{\rho}(\theta, \alpha; t)|W\rangle}$ is the fidelity between $\hat{\rho}(\theta, \alpha; t)$ and the W-state. For arbitrarily small values of α such as 0.01, if we choose $\theta = \pi$ the expectation values of $\hat{W}'$ with respect to $\hat{\rho}(\pi, 0.01; t))$ for some times t^* becomes $-1/3$, as shown in Fig. 4 and Fig. 5, which means that $F(|W\rangle\langle W|, \hat{\rho}(\pi, 0.01; t^*)) \simeq 1$. Consequently, by the dynamics of the system, the excitonic modes of three QDs construct entangled coherent W-state, the other type of tripartite entangled coherent state which are not equivalent to the GHZ-state [33]. Also, it can be obtained the average number of photons in the field modes of cavities as follows

$$\langle n_c \rangle = \frac{(1 + e^{-2|\alpha|^2})|\alpha|^2(|u_{21}(t)|^2 + 2|u_{22}(t)|^2)}{1 - e^{-2|\alpha|^2}}, \tag{15}$$

where for resonance and nonresonance interaction regimes, has been sketched in the Fig. 4 and Fig. 5 respectively. On the other hand, in the presence of resonance interaction between photons and excitons, for both cases of construction of entangled coherent GHZ and W states, the field modes of cavities highly populated as shown in the Fig. 2 and Fig. 4. This means that in the presence of interaction between the cavity system and environment, it is evident from [31, 32] that: the larger the average number of photons inside the cavities, the faster will the coherence decay. Therefore, decoherency aspects of the system dominates to coherency one and therefore the suggested protocol for generation of entanglement is not utilizable. One of the essential improvement in robust construction of entanglement using a system of coupled cavities is the prevention of populating of the field mode in the cavities [5]. To this end, we see that in the nonresonance interaction regime ($\Delta \neq 0$), the average number of photons in the field mode of the cavities can become a vanishing amount as depicted in Fig. 3 and Fig. 5. Therefore, in the nonresonance regime, during the process of generating entanglement between excitons of QDs in the cavities which takes place slowly rather than to the resonance case, the field mode of each cavity is approximately at the respective vacuum state [5, 34, 35]. In another words, generating entanglement between the excitonic modes in distant QDs, can be done by negligible populations of the field modes in the coupled-cavity system, protecting against decoherence via related decays of cavities.

4 Explicit evaluation of decoherence effect on the entanglement

Decoherences and environmental losses are important effects in quantum information processing [18]. In the presence of Decoherences, the system due to the coupling to its environment is open and its dynamics, consists of two coherent and incoherent parts, can be described within the framework of master equations of Lindblad form [36]. The system considered in this paper (Fig. 1.) can be subjected to several dissipative processes as sources of decoherence, such as cavities losses at decay rates γ_{c_i}s ($i = 1, 2, 3$), which in turn, arise due to interaction of the field mode in each cavity with a common reservoir [37]. Also, another dissipations are related to the interaction of excitons in the QDs with the same reservoir at rates γ_{e_i}s ($i = 1, 2, 3$). Since the three cavities are equivalent and so the QDs, we take $\gamma_c := \gamma_{c_1} = \gamma_{c_2} = \gamma_{c_3}$ and $\gamma_e := \gamma_{e_1} = \gamma_{e_2} = \gamma_{e_3}$. Hence, in the schrodinger picture, the time evolution of the whole system is described by the following master equation for the density operator $\hat{\rho}$ as

$$\begin{aligned}\dot{\hat{\rho}} = i[\hat{\rho}, \hat{H}] + \sum_{i=1}^{3} \left(2\hat{L}_{c_i}\rho\hat{L}_{c_i}^{\dagger} - \hat{L}_{c_i}\hat{L}_{c_i}^{\dagger}\hat{\rho} - \hat{\rho}\hat{L}_{c_i}\hat{L}_{c_i}^{\dagger}\right) \\ + \sum_{i=1}^{3} \left(2\hat{L}_{e_i}\rho\hat{L}_{e_i}^{\dagger} - \hat{L}_{e_i}\hat{L}_{e_i}^{\dagger}\hat{\rho} - \hat{\rho}\hat{L}_{e_i}\hat{L}_{e_i}^{\dagger}\right),\end{aligned} \tag{16}$$

where $\hat{L}_{c_i} = \sqrt{\gamma_c}\ \hat{a}_i$ and $\hat{L}_{e_i} = \sqrt{\gamma_e}\ \hat{b}_i$ with $i = 1, 2, 3$, are the Lindblad operators corresponding to the cavity field modes and the excitons of QDs and $\hat{H}$ is the Hamiltonian of the system introduced in Eq. 1. If we transfer the description into the Heisenberg picture, the time evolution of a typical operator of the system such as $\hat{O}$, is obtained by the following equation [36, 38],

$$\begin{aligned}\dot{\hat{O}} = -i[\hat{O}, \hat{H}] + \sum_{i=1}^{3} \left(2\hat{L}_{c_i}^{\dagger}\hat{O}\hat{L}_{c_i} - \hat{L}_{c_i}^{\dagger}\hat{L}_{c_i}\hat{O} - \hat{O}\hat{L}_{c_i}^{\dagger}\hat{L}_{c_i}\right) \\ + \sum_{i=1}^{3} \left(2\hat{L}_{e_i}^{\dagger}\hat{O}\hat{L}_{e_i} - \hat{L}_{e_i}^{\dagger}\hat{L}_{e_i}\hat{O} - \hat{O}\hat{L}_{e_i}^{\dagger}\hat{L}_{e_i}\right).\end{aligned} \tag{17}$$

In the right hand side of the Eq. 17, the first term represents the coherent or unitary evolution of the operator and the next terms show the incoherent or dissipative ones. Eq. 17, for the operators $\hat{a}_i$s and $\hat{b}_i$s ($i = 1, 2, 3$), gives the set of first order differential equations similar to the Eq. 2, except that we should consider $\omega_c \to \omega_c - i\gamma_c$ and $\Delta \to \Delta + i(\gamma_e - \gamma_c)$. By considering these replacements, the solutions of the set of differential equations for the operators $\hat{a}_i(t)$s and $\hat{b}_i(t)$s ($i = 1, 2, 3$) of the open system, are obtain analytically as obtained for its closed counterpart discussed in the section 2. Now by considering the initial state in Eq. 5, in the presence of related dissipations, the time evolution of the reduced density matrix for excitonic modes of three QDs namely $\hat{\rho}_{_{diss}}(\theta, \alpha; t)$, in similar way as for $\hat{\rho}(\theta, \alpha; t)$ in Eq. 8, is obtained. The expectation values of the witness operator $\hat{W}$ with respect to the density matrix $\hat{\rho}_{_{diss}}(0, 2; t)$, that is, $E_{_{GHZ}}\left(\hat{\rho}_{_{diss}}(0, 2; t)\right)$ with $\gamma_e = 0.001$ and $\gamma_c = 0$, at the resonance and nonresonance cases have been shown in Fig. 6 and Fig. 7 respectively. As it is evident, the existence of losses of excitons in QDs destroys the entanglement of

coherent GHZ-states generated in both resonance and nonresonance cases. However, when the photon losses in the cavities are included (for example with $\gamma_c = 0.05$), the destruction rates of the entanglement for the resonance and nonresonance cases are considerably different as shown in Fig. 8 and Fig. 9. It is obvious that the entanglement in the nonresonance case is more robust due to the photon losses in the cavities than the resonance case. In fact, as discussed in the previous section, the negligible populations of the field modes in the cavities at the nonresonance regime suppresses the destruction of the entanglement due to the photon loesses. On the other hand, similar observations are obtained in constructing entangled coherent W-state by considering the same dissipation processes as it can be seen in the Fig. 10, Fig. 11, Fig. 12, Fig. 13.

5 Conclusions

We have presented a protocol for robust construction of entangled coherent GHZ and W states between the excitonic modes of three QDs trapped in coupled-cavity system. This protocol utilizes the cavity field, induced nonlocal interaction, to couple three QDs for establishing tripartite entanglement between created excitons. As illustrated by the master equation approach, the negligible populations of the field modes in the cavity system suppress efficiently the effect of photon losses on the generated entanglement.

Appendix:

The solutions of (2) for $\hat{a}_2(t)$, $\hat{a}_3(t)$ and $\hat{b}_1(t)$, $\hat{b}_2(t)$ and $\hat{b}_3(t)$ are given as follow:

$$\hat{a}_1(t) = u_{11}(t)\hat{a}_1(0) + u_{12}(t)(\hat{a}_2(0) + \hat{a}_3(0)) + v_{11}(t)\hat{b}_1(0) + v_{12}(t)(\hat{b}_2(0) + \hat{b}_3(0)), \tag{1}$$

$$\hat{a}_2(t) = u_{11}(t)\hat{a}_2(0) + u_{12}(t)(\hat{a}_1(0) + \hat{a}_3(0)) + v_{11}(t)\hat{b}_2(0) + v_{12}(t)(\hat{b}_1(0) + \hat{b}_3(0)), \tag{2}$$

$$\hat{a}_3(t) = u_{11}(t)\hat{a}_3(0) + u_{12}(t)(\hat{a}_1(0) + \hat{a}_2(0)) + v_{11}(t)\hat{b}_3(0) + v_{12}(t)(\hat{b}_1(0) + \hat{b}_2(0)), \tag{3}$$

$$\hat{b}_2(t) = u_{21}(t)\hat{a}_2(0) + u_{22}(t)(\hat{a}_1(0) + \hat{a}_3(0)) + v_{21}(t)\hat{b}_2(0) + v_{22}(t)(\hat{b}_1(0) + \hat{b}_3(0)), \tag{4}$$

$$\hat{b}_3(t) = u_{21}(t)\hat{a}_3(0) + u_{22}(t)(\hat{a}_1(0) + \hat{a}_2(0)) + v_{21}(t)\hat{b}_3(0) + v_{22}(t)(\hat{b}_1(0) + \hat{b}_2(0)), \tag{5}$$

where $u_{1j}(t)$ and $v_{1j}(t)$ for $j = 1, 2$ are denoted as

$$\begin{aligned}
u_{11}(t) &= \tfrac{e^{-i\omega_c t}}{3}\left(e^{-i(c-\frac{\Delta}{2})t}(cos(\tfrac{At}{2}) - \tfrac{i(2c+\Delta)}{A}sin(\tfrac{At}{2})) + 2e^{i(\frac{c+\Delta}{2})t}(cos(\tfrac{Bt}{2}) + \tfrac{i(c-\Delta)}{B}sin(\tfrac{Bt}{2}))\right)\\
u_{12}(t) &= \tfrac{e^{-i\omega_c t}}{3}\left(e^{-i(c-\frac{\Delta}{2})t}(cos(\tfrac{At}{2}) - \tfrac{i(2c+\Delta)}{A}sin(\tfrac{At}{2})) - e^{i(\frac{c+\Delta}{2})t}(cos(\tfrac{Bt}{2}) + \tfrac{i(c-\Delta)}{B}sin(\tfrac{Bt}{2}))\right)\\
v_{11}(t) &= \tfrac{ie^{-i\omega_c t}}{6g}\left(e^{-i(c-\frac{\Delta}{2})t}(-A + \tfrac{(2c+\Delta)^2}{A})sin(\tfrac{At}{2}) - 2e^{i(\frac{c+\Delta}{2})t}(B - \tfrac{(c-\Delta)^2}{B})sin(\tfrac{Bt}{2})\right)\\
v_{12}(t) &= \tfrac{ie^{-i\omega_c t}}{6g}\left(e^{-i(c-\frac{\Delta}{2})t}(-A + \tfrac{(2c+\Delta)^2}{A})sin(\tfrac{At}{2}) + e^{i(\frac{c+\Delta}{2})t}(B - \tfrac{(c-\Delta)^2}{B})sin(\tfrac{Bt}{2})\right)
\end{aligned} \tag{6}$$

References

[1] J. I. Cirac, A. K. Ekert, S. F. Huelga, and C. Macchiavello, Phys. Rev. A 59, 4249 (1999).

[2] M. Hartmann, F.G.S.L. Brandao, M.B. Plenio, Nat. Phys. 2, 849 (2006).

[3] D. G. Angelakis, M. F. Santos and S. Bose, Phys. Rev. A 76, 031805(R) (2007).

[4] L. Lamata, D. R. Leibrandt, I. L. Chuang, J. I. Cirac, M. D. Lukin, V. Vuletic and S. F. Yelin, Phys. Rev. Lett. 107, 030501 (2011).

[5] C.D. Ogden, E.K. Irish, M.S. Kim, Phys. Rev. A 78, 063805 (2008).

[6] P. B. Li, Y. Gu, Q. H. Gong, and G. C. Guo, Phys. Rev. A 79, 042339 (2009).

[7] B. F. C. Yabu-uti, J. A. Roversi, Quantum Inf Process 12, 189 (2013).

[8] J. I. Cirac, P. Zoller, H. J. Kimble, and H. Mabuchi, Phys. Rev. Lett. 78, 3221 (1997).

[9] K. Hennessy, A. Badolato, M. Winger, D. Gerace, M. Atature, S. Gulde, S. Falt, E.L. Hu, A. Imamoglu, Nature 445, 896 (2007).

[10] G. Khitrova, H.M. Gibbs, M. Kira, W. Kochs, A. Scherer, Nat. Phys. 2, 81 (2006).

[11] Z.R. Zhong, Opt. Commun. 283, 1972 (2010).

[12] X.L. Feng, Z.M. Zhang, X.D. Li, Phys. Rev. Lett. 90, 217902 (2003).

[13] T. Pellizzari, Phys. Rev. Lett. 79, 5242 (1997).

[14] A. Serafini, S. Mancini, S. Bose, Phys. Rev. Lett. 96, 010503 (2006).

[15] B. Bellomo, G. Compagno, R. Lo Franco, A. Ridolfo and S. Savasta, Phys. Scr. 2011, 014004 (2011).

[16] D. M. Greenberger, M. Horne, and A. Zeilinger, in Bells Theorem, Quantum Theory, and Conceptions of the Universe, edited by M. Kafatos (Kluwer, Dordrecht, 1989).

[17] [2] J. W. Pan, D. Bouwmeester, M. Daniell, H. Weinfurter, and A. Zeilinger, Nature (London) 403, 515 (2000).

[18] R. Chen, L. Shen, Phys. Lett. A 375, 3840 (2011).

[19] W.-A. Li and L.-F. Wei, OPTICS EXPRESS 20, 13440 (2012).

[20] X.-Y. Lu, L.-G. Si, X.-Y. Hao, X. Yang, Phys. Rev. A 79, 052330 (2009)

[21] W. Duer, G. Vidal, and J. I. Cirac, Phys. Rev. A 62, 062314 (2000).

[22] J. Kempe, Phys. Rev. A 60, 910 (1999); A. V. Thapliyal, ibid. 59, 3336 (1999); D. Gottesman and I. L. Chuang, Nature (London) 402, 390 (1999); M. A. Nielsen and I. L. Chuang, Quantum Computation and Quantum Information (Cambridge University Press, Cambridge, 2000).

[23] B. C. Sanders, Phys. Rev. A 45, 6811 (1992).

[24] A. P. Lund, T. C. Ralph, and H. L. Haselgrove, Phys. Rev. Lett. 100, 030503 (2008).

[25] N. B. An, Phys. Lett. A 373, 1701 (2009).

[26] P. Marek and J. Fiurasek, Phys. Rev. A 82, 014304 (2010).

[27] H. Jeong, N. B. An, Phys. Rev. A 74, 022104 (2006).

[28] N. B. An, Phys. Rev. A 69, 022315 (2004).

[29] A. Acin, D. Brus, M. Lewenstein, A. Sanpera, Phys. Rev. Lett. 87, 040401 (2001).

[30] M. Bourennance, M. Eibl, C. Kurtsiefer, S. Gaertner, H. Weinfurter, O. Guhne, P. Hyllus, D. Brus, M. Lewenstein, A. Sanpera, Phys. Rev. Lett. 92, 087902 (2004).

[31] L. Davidovich, M. Brune, J. M. Raimond, and S. Haroche, Phys. Rev. A 53, 1295 (1996).

[32] K. M. Fonseca Romero, M. C. Nemes, J. G. Peixoto de Faria, A. N. Salgueiro, and A. F. R. de Toledo Piza, Phys. Rev. A 58, 3205 (1998).

[33] X. Wang and B. C. Sanders, Phy. Rev. A 65, 012303 (2001).

[34] S.B. Zheng, G.C. Guo, Phys. Rev. Lett. 85, 2392 (2000).

[35] J. Majer et al., Nature 449, 443 (2007).

[36] C. Gardiner and P. Zoller, Quantum Noise, Springer (2004).

[37] W. H. Louisell and W. H. Marburger, IEEE J. Quantum Electron. 3, 348 (1967).

[38] M. J. Hartmann, J. Prior, S. R. Clark, and M. B. Plenio, Phys. Rev. Lett. 102, 057202 (2009).

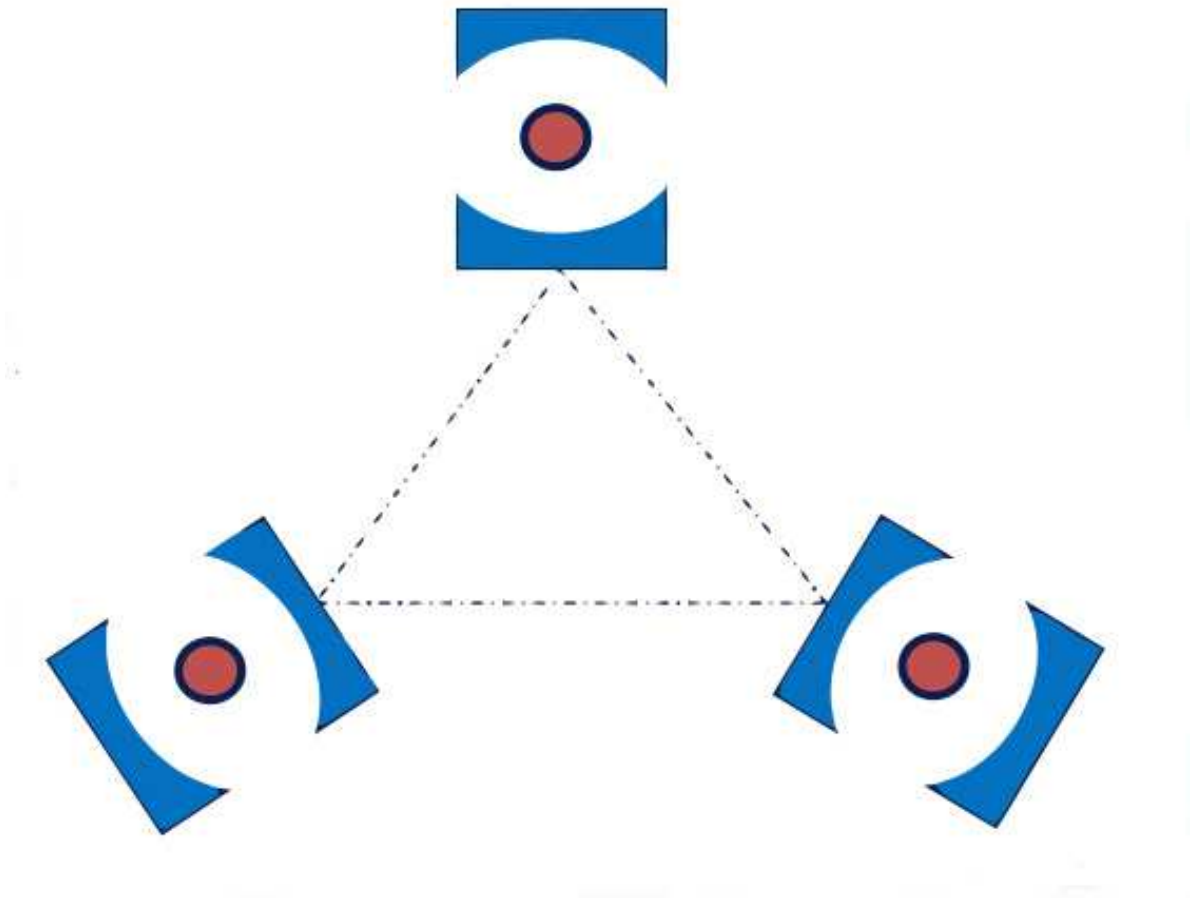

Figure 1:

Figure Captions

- Fig. 1. Three optical cavities each of which is doped with a QD, coupled to each other through photon hopping.

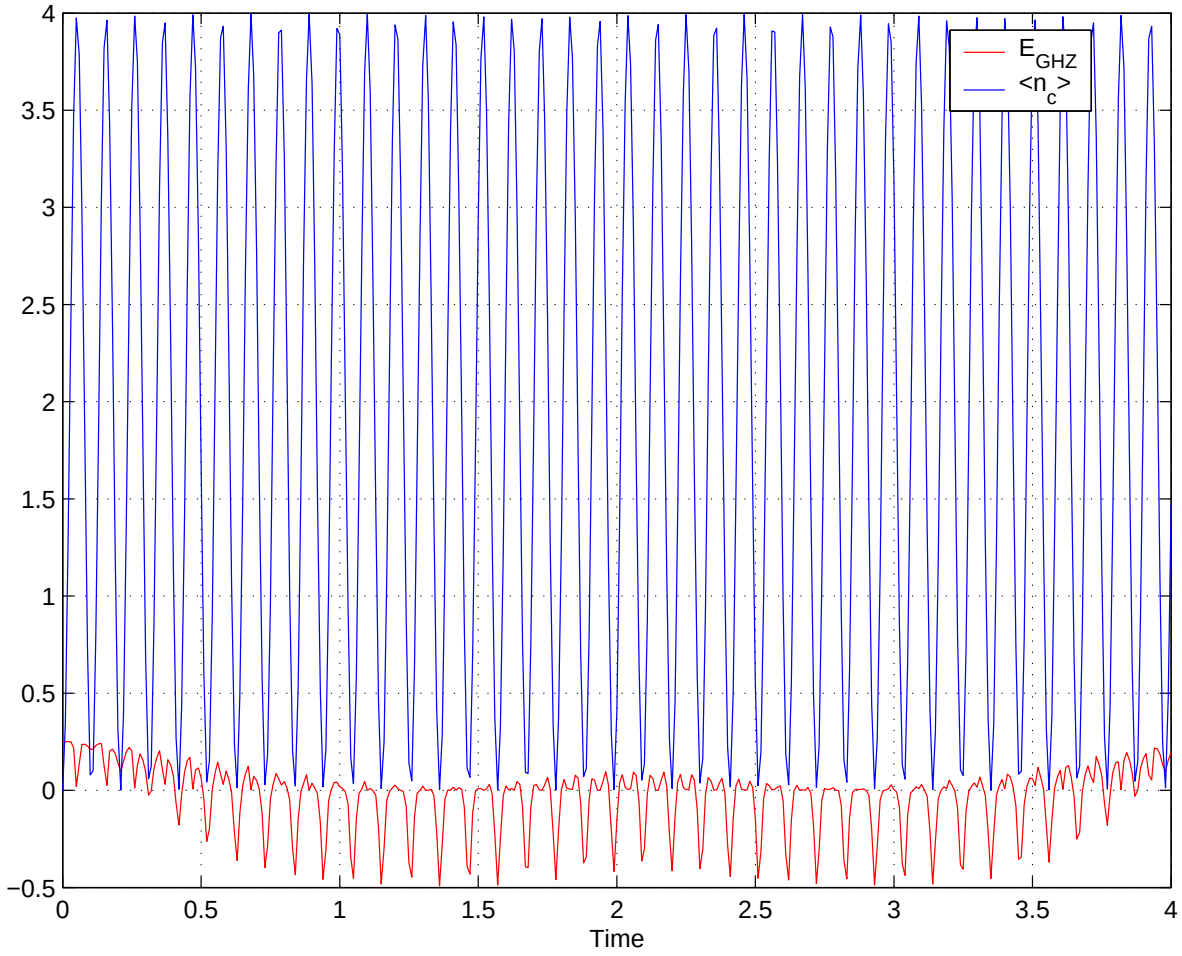

Figure 2:

Figure Captions

– Fig. 2. $E_{GHZ}\left(\hat{\rho}(0,2;t)\right)$ and the related average number of photons ($< \mathrm{n_c} >$) for $c = 1$, $g = 30$ and $\Delta = 0$.

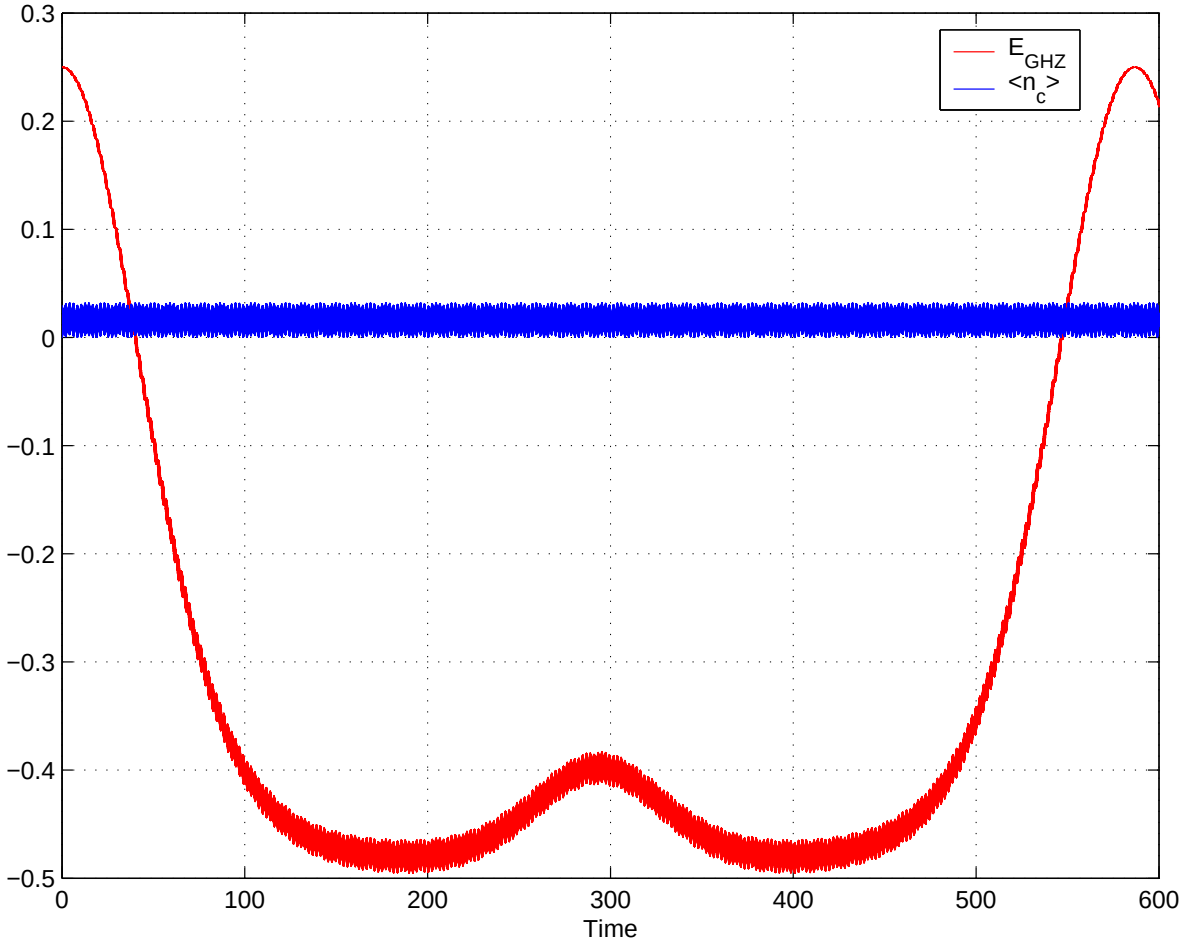

Figure 3:

Figure Captions

∗ Fig. 3. $E_{GHZ}\,(\hat{\rho}(0,2;t))$ and the related average number of photons ($<\mathrm{n_c}>$) for $c=1$, $g=30$ and $\Delta=-500$.

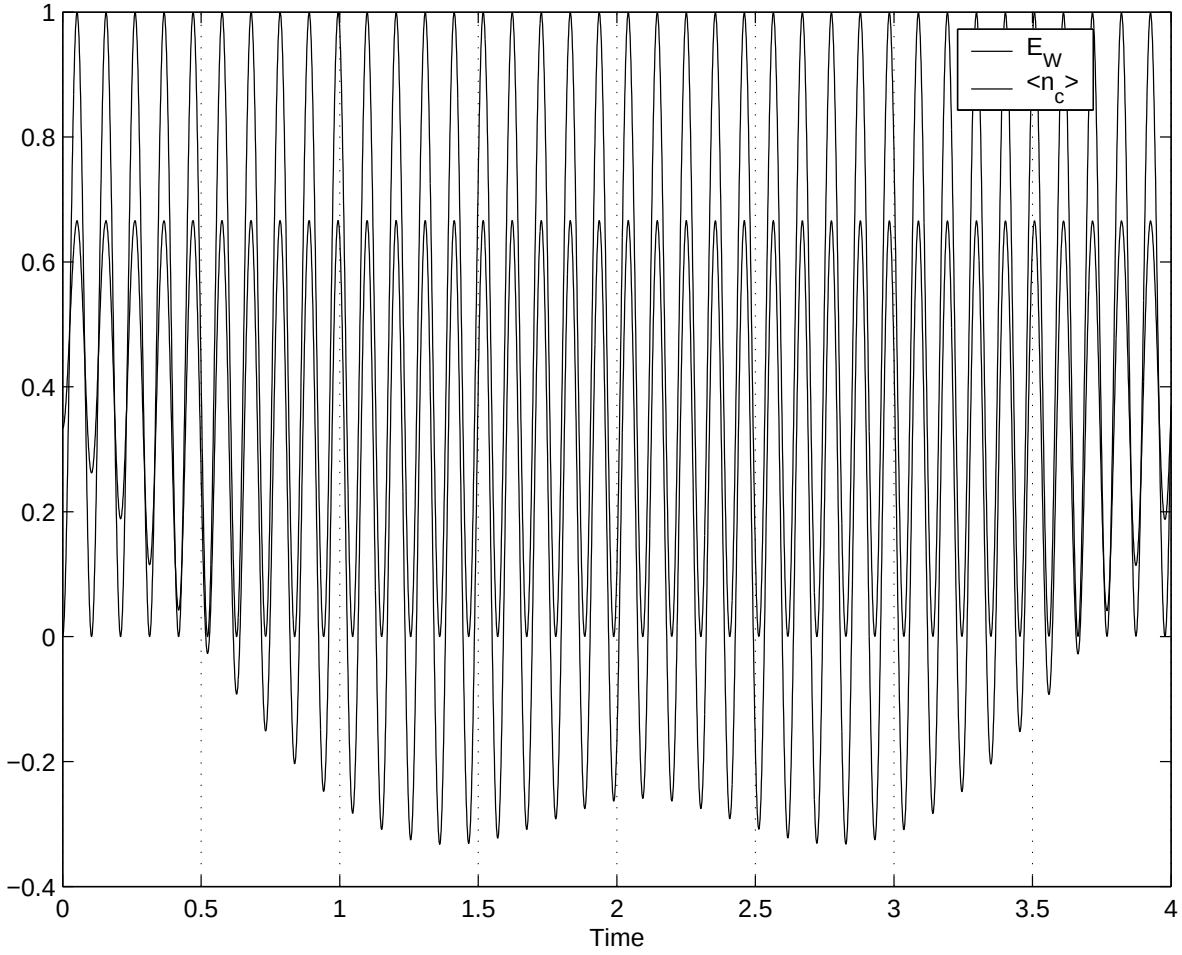

Figure 4:

Figure Captions

· Fig. 4. $E_W\,(\hat{\rho}(\pi, 0.01; t))$ and the related average number of photons ($< \mathrm{n_c} >$) for $c = 1$, $g = 30$ and $\Delta = 0$.

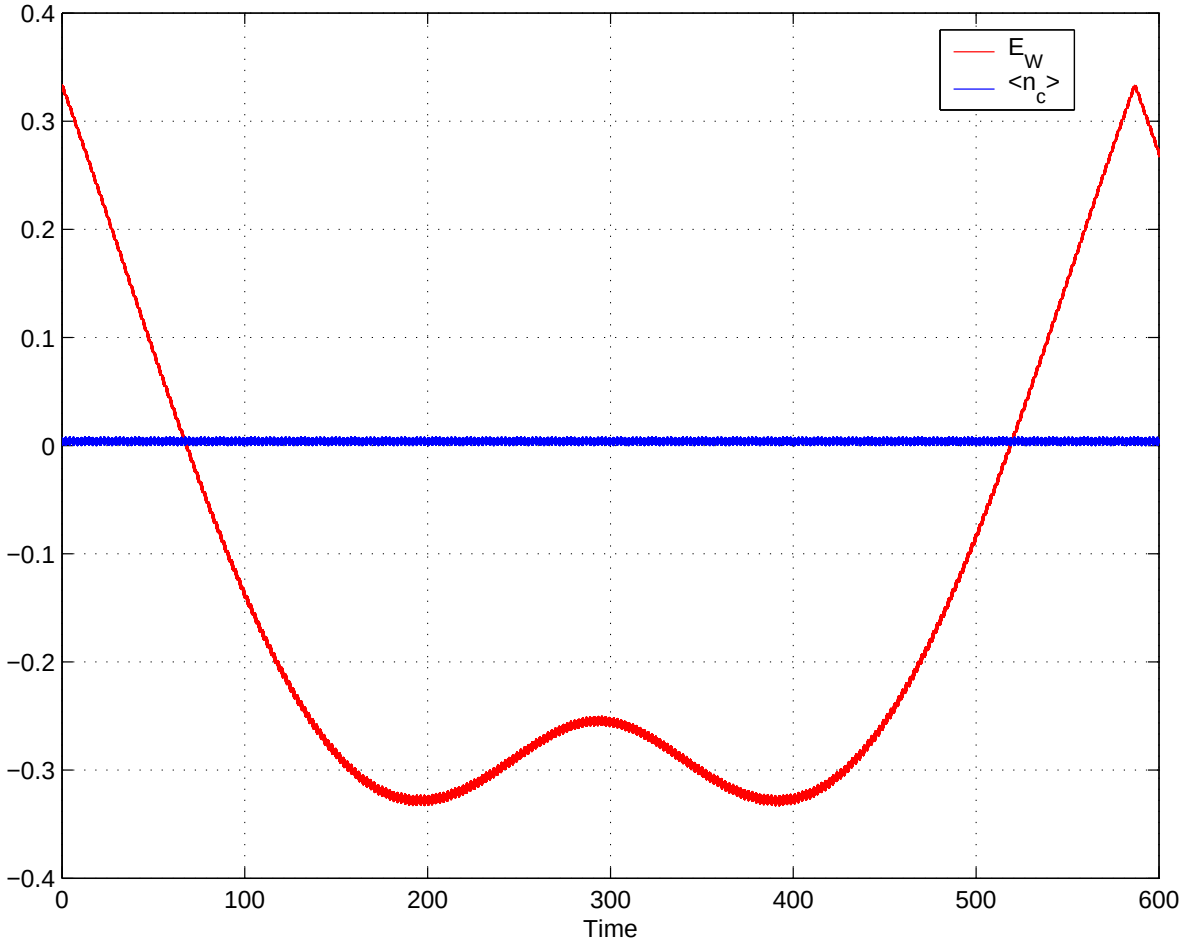

Figure 5:

Figure Captions

· Fig. 5. $E_W\,(\hat{\rho}(\pi, 0.01; t))$ and the related average number of photons ($< \mathrm{n_c} >$) for $c = 1$, $g = 30$ and $\Delta = -500$.

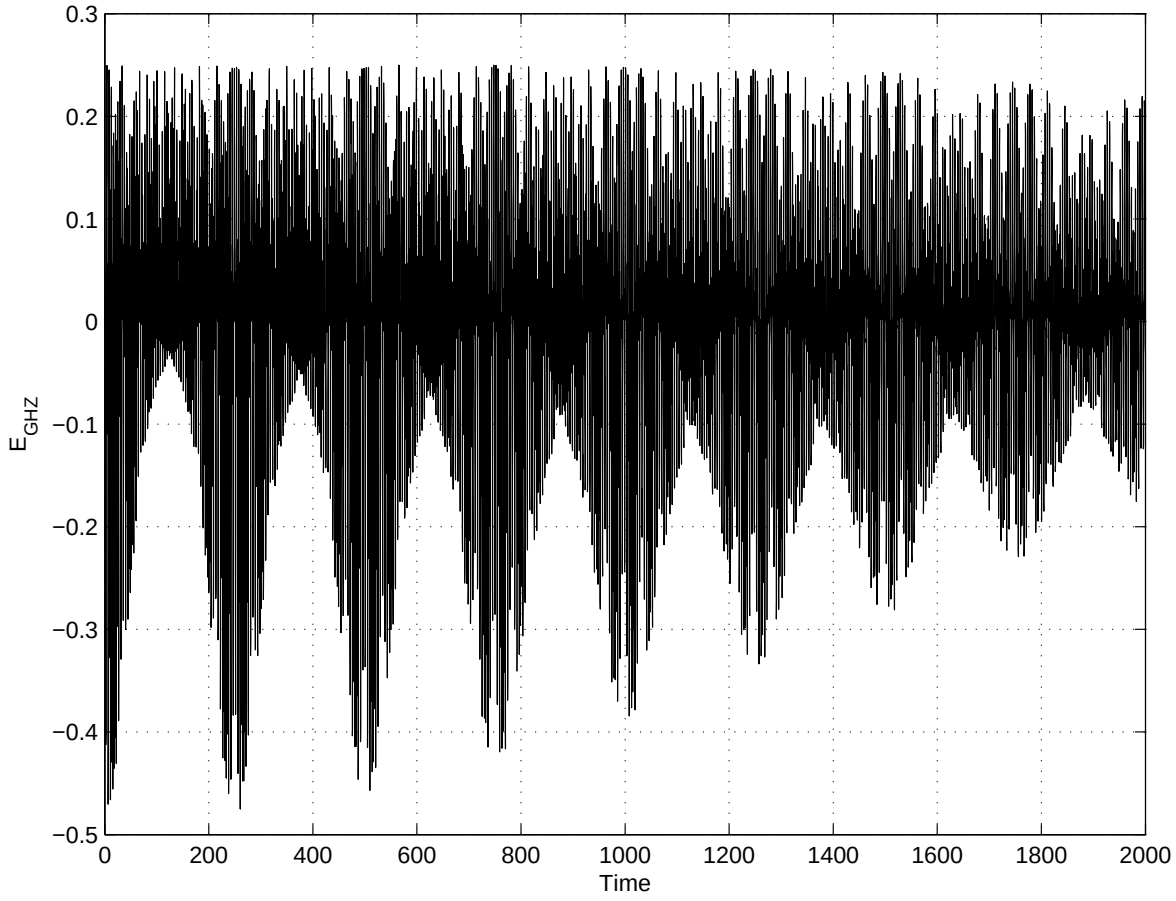

Figure 6:

Figure Captions

· Fig. 6. $E_{GHZ}\left(\hat{\rho}_{diss}(0,2;t)\right)$ for $c = 1$, $g = 30$, $\Delta = 0$, $\gamma_e = 0.001$ and $\gamma_c = 0$.

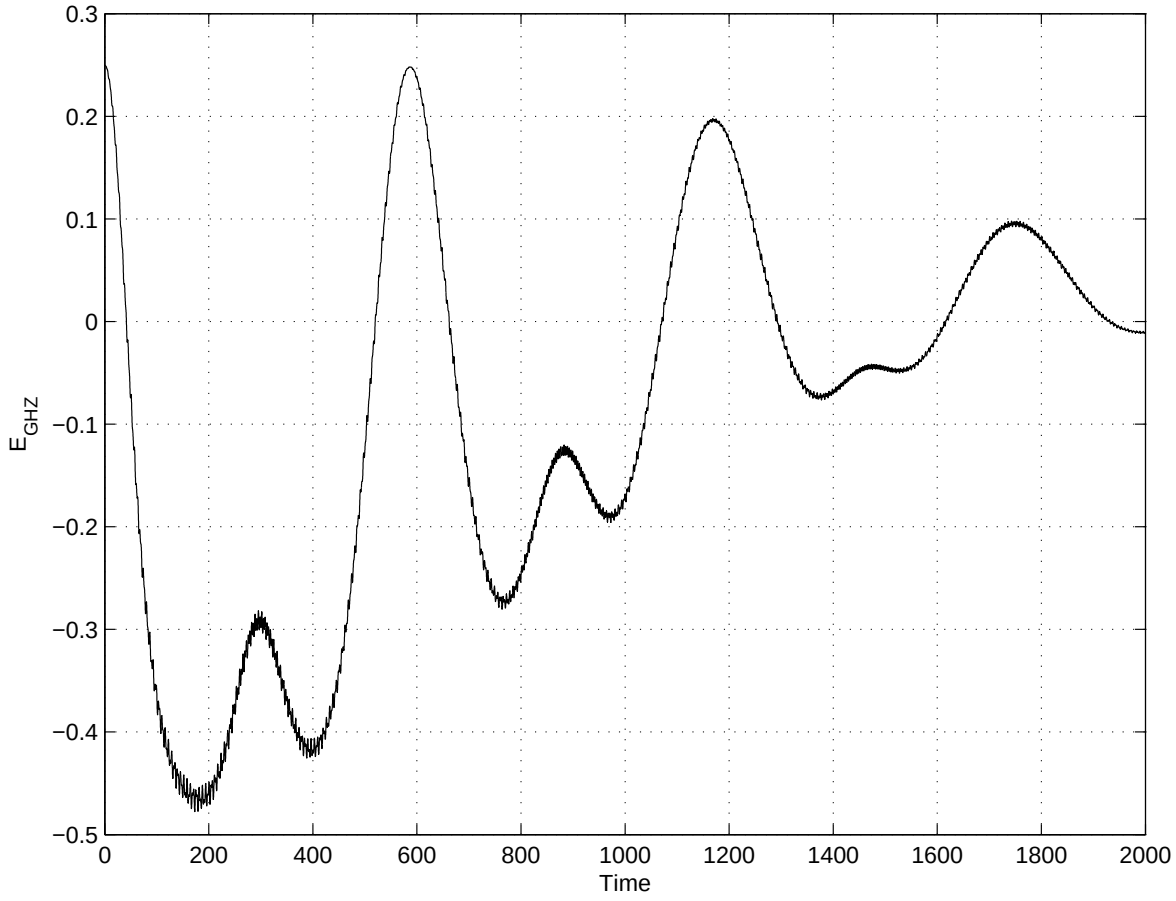

Figure 7:

Figure Captions

· Fig. 7. $E_{GHZ}\left(\hat{\rho}_{diss}(0,2;t)\right)$ for $c=1$, $g=30$, $\Delta=-500$, $\gamma_e=0.001$ and $\gamma_c=0$.

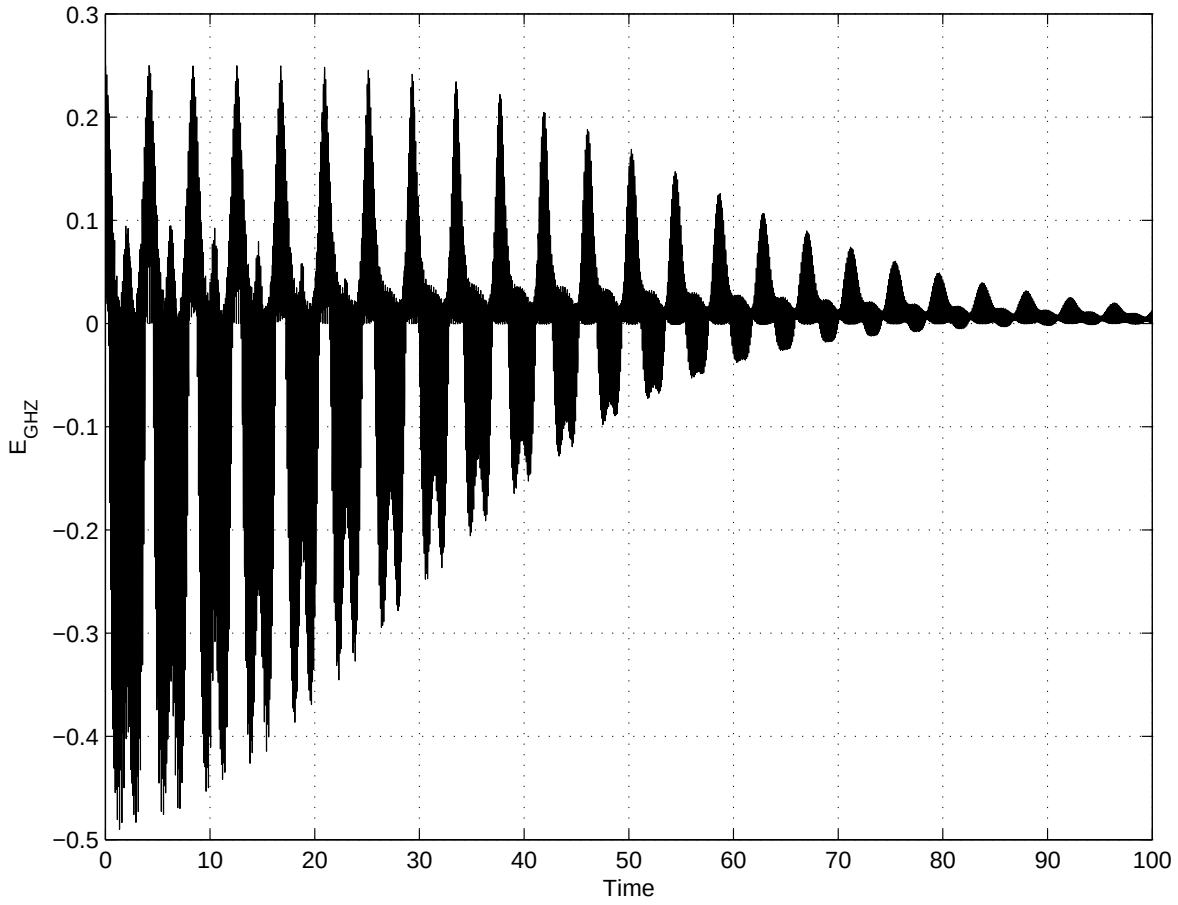

Figure 8:

Figure Captions

· Fig. 8. $E_{GHZ}\left(\hat{\rho}_{diss}(0,2;t)\right)$ for $c = 1$, $g = 30$, $\Delta = 0$, $\gamma_e = 0.001$ and $\gamma_c = 0.05$. The destruction of the generated entangled coherent GHZ-state is considerable in comparison to the case that the photon losses in the cavities are not included (see Fig. 6).

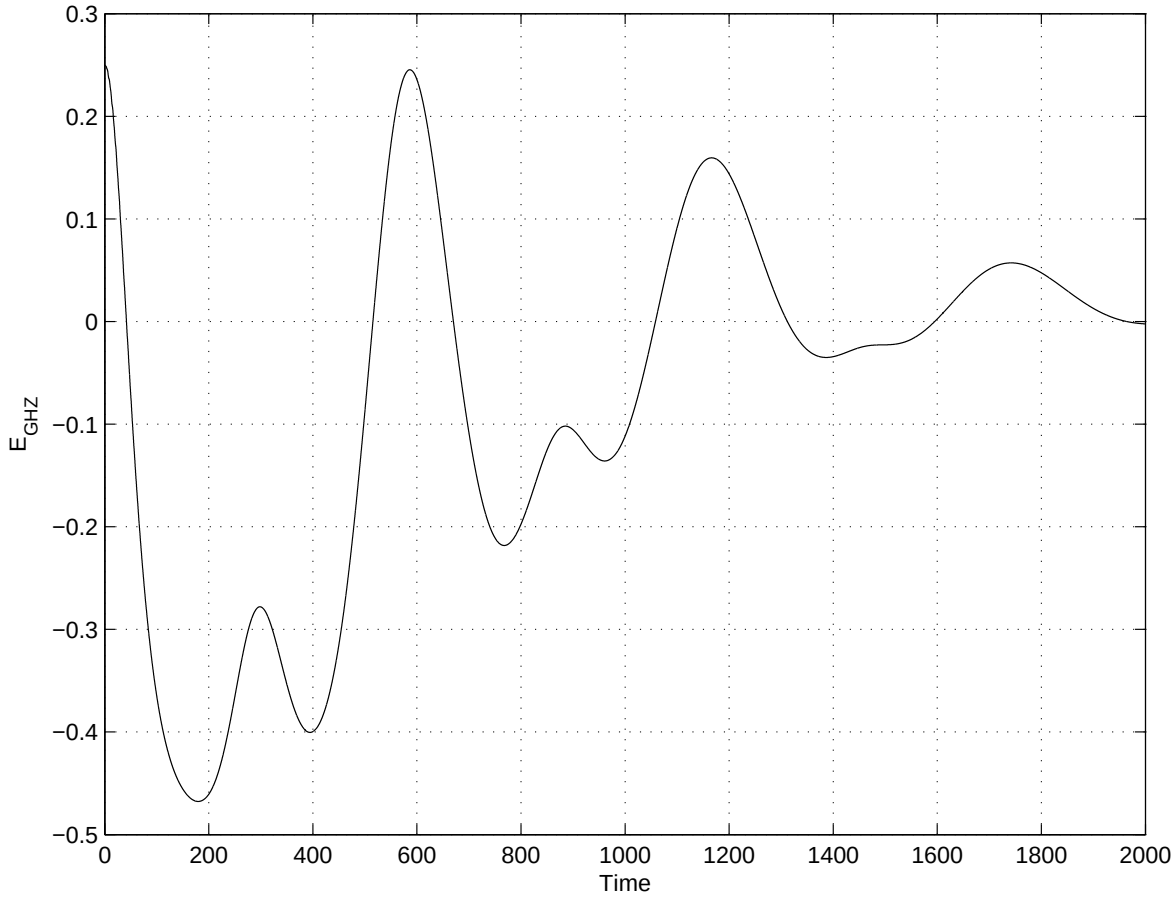

Figure 9:

Figure Captions

· Fig. 9. $E_{GHZ}\left(\hat{\rho}_{diss}(0,2;t)\right)$ for $c=1$, $g=30$, $\Delta=-500$, $\gamma_e=0.001$ and $\gamma_c=0.05$. For this case, obviously the robustness of entanglement due to the photon losses in the cavities is considerably more than one in the resonance case.

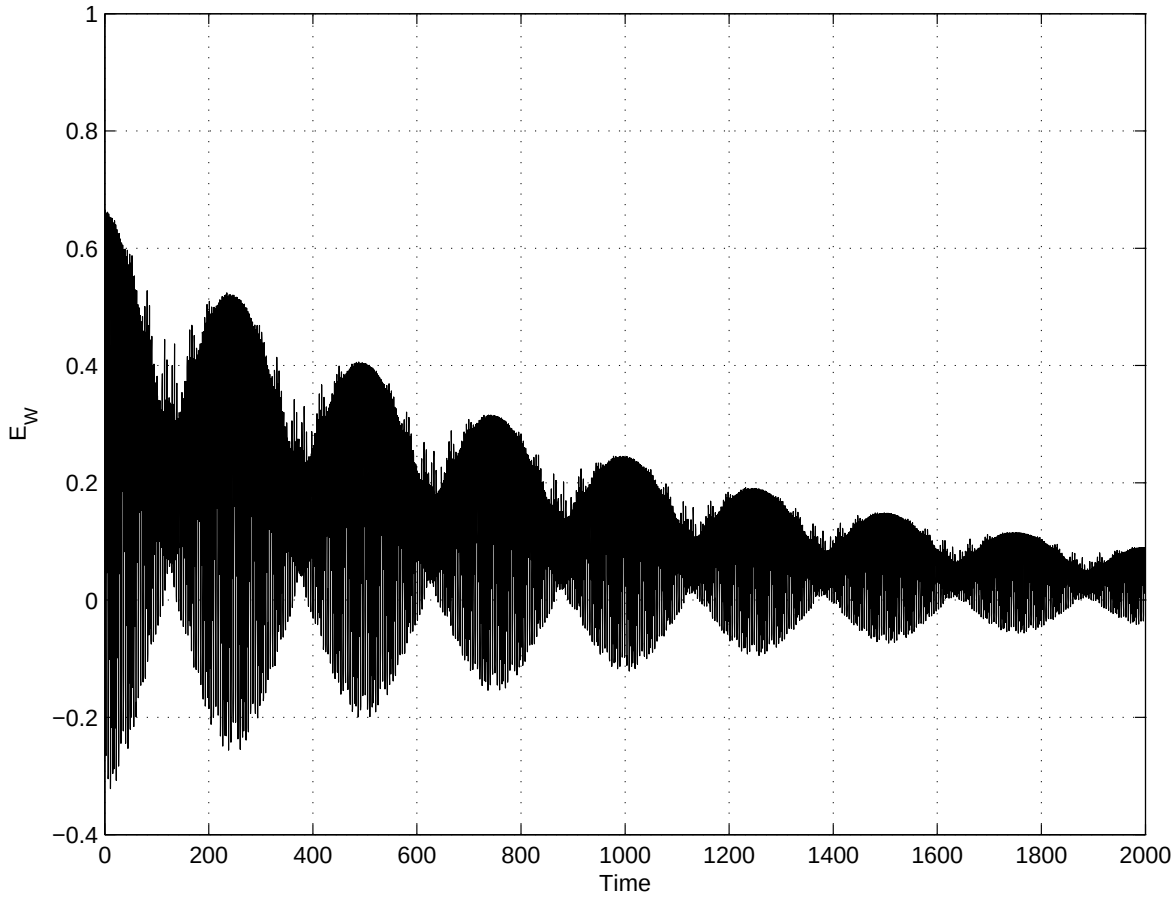

Figure 10:

Figure Captions

· Fig. 10. $E_W\left(\hat{\rho}_{diss}(\pi, 0.01; t)\right)$ for $c = 1$, $g = 30$, $\Delta = 0$, $\gamma_e = 0.001$ and $\gamma_c = 0$.

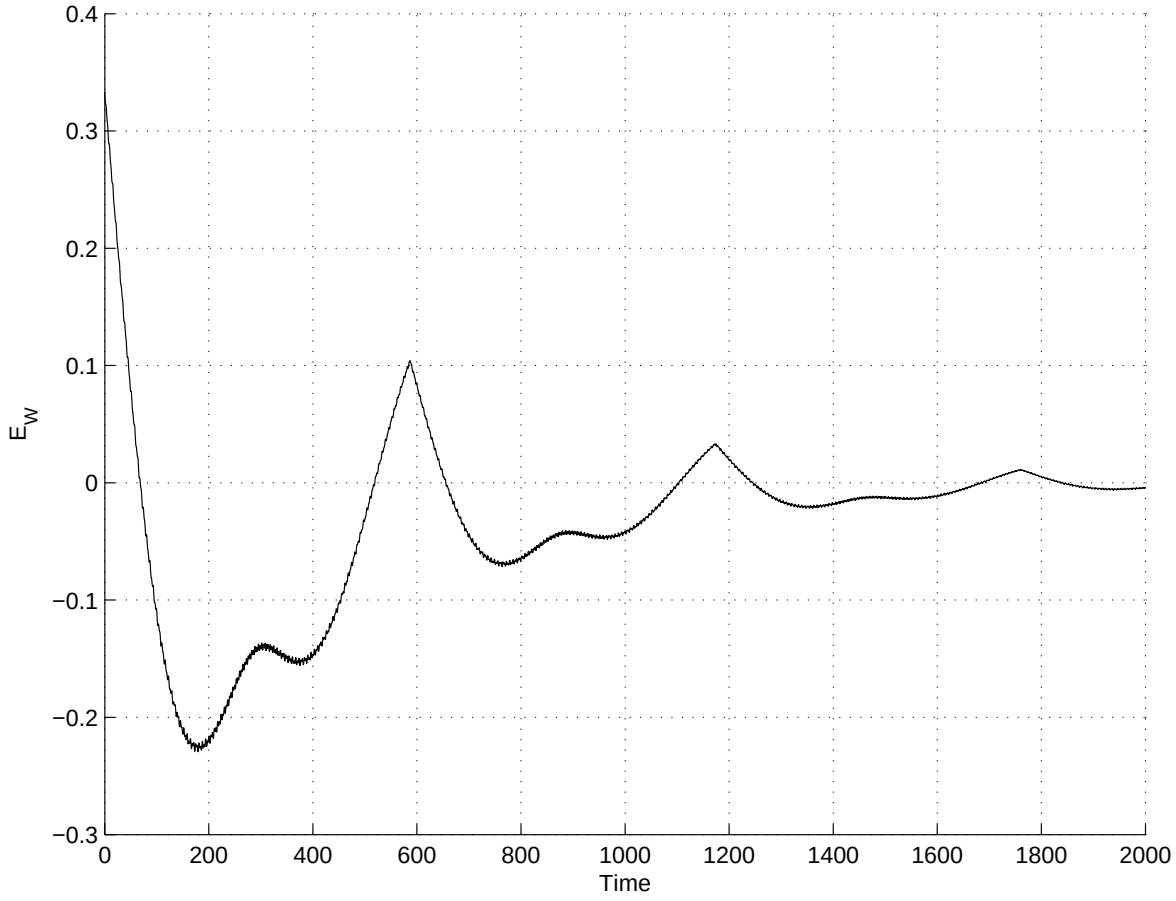

Figure 11:

Figure Captions

· Fig. 11. $E_W\left(\hat{\rho}_{diss}(\pi, 0.01; t)\right)$ for $c = 1$, $g = 30$, $\Delta = -500$, $\gamma_e = 0.001$ and $\gamma_c = 0$.

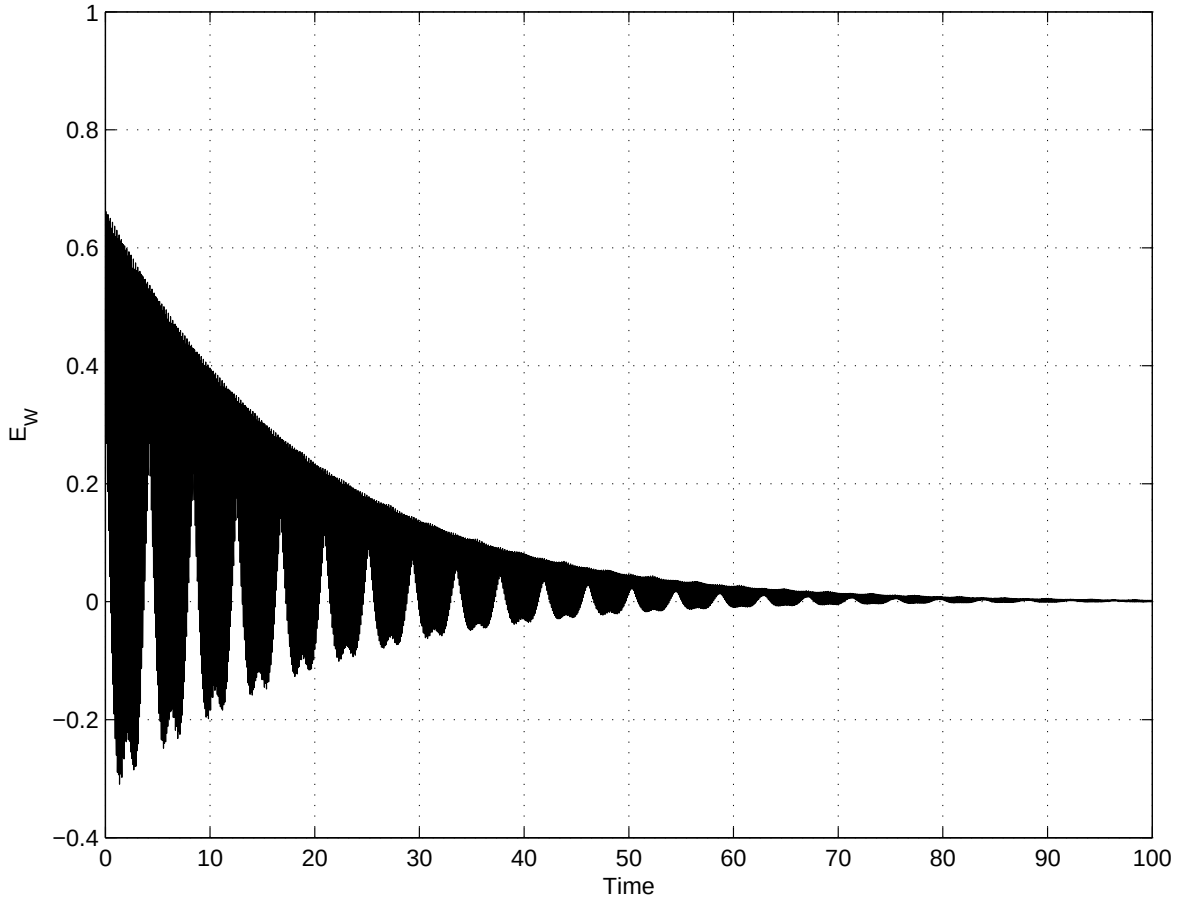

Figure 12:

Figure Captions

· Fig. 12. $E_{_W}\left(\hat{\rho}_{_{diss}}(\pi, 0.01; t)\right)$ for $c = 1$, $g = 30$, $\Delta = 0$, $\gamma_e = 0.001$ and $\gamma_c = 0.05$. Obviously, with these parameters, the destruction rate of the entanglement of coherent W-state due to the photon losses in the cavities is even more than one of the coherent GHZ-state as shown in Fig. 8.

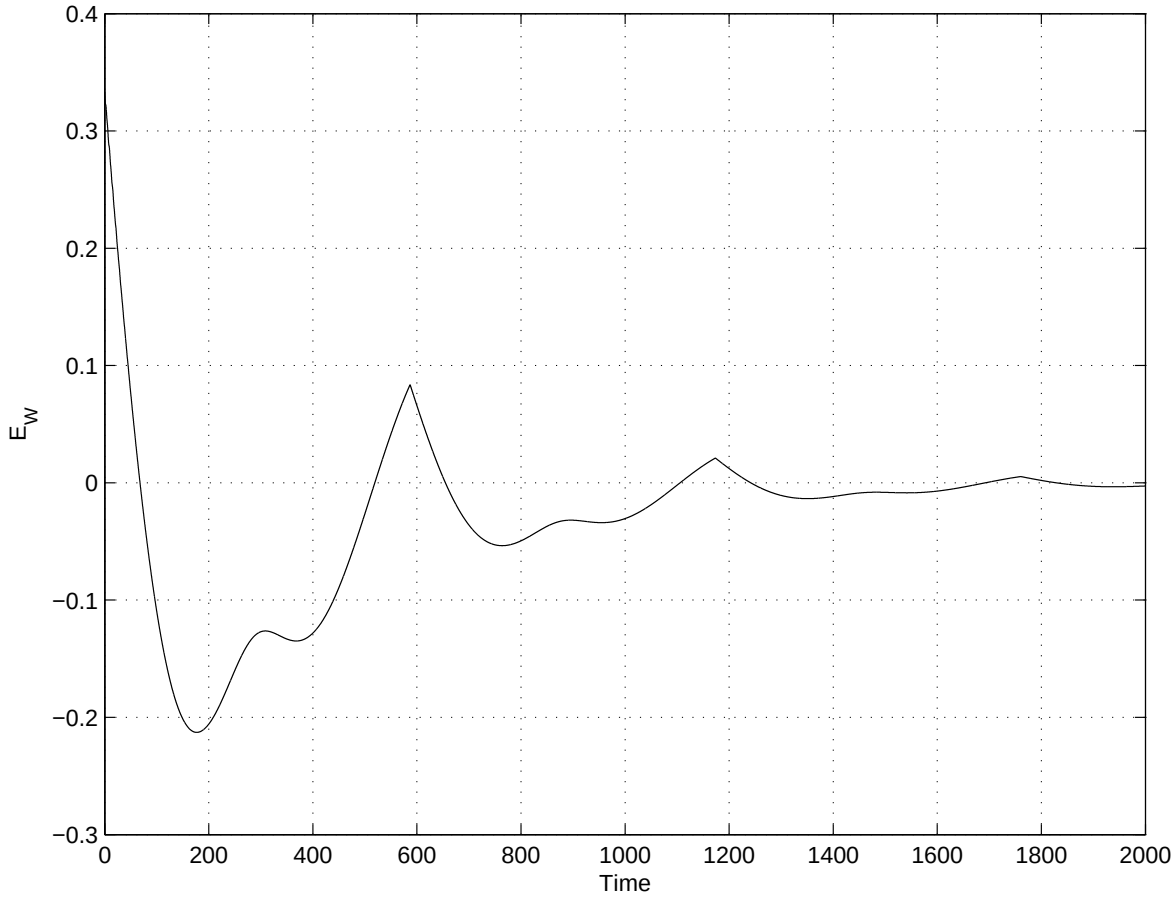

Figure 13:

Figure Captions

· Fig. 13. $E_{_W}\left(\hat{\rho}_{_{diss}}(\pi, 0.01; t)\right)$ for $c = 1$, $g = 30$, $\Delta = -500$, $\gamma_e = 0.001$ and $\gamma_c = 0.05$. It is clearly observed that the robustness of entanglement of coherent W-state due to the photon losses in the cavities for nonresonance regime is considerably more than one for the resonance regime as depicted in Fig. 12.